

Application of Exact Synthesis Methods to Multichannel Filter Design

R. J. WENZEL, MEMBER IEEE

Abstract—An exact design procedure is presented for contiguous-band multichannel filters. The procedure is theoretically valid at all frequencies for filters which employ TEM-mode (transverse-electromagnetic-mode), quarter-wave line networks. The design of diplexing networks is considered in detail with multichannel filters being realized as a cascade of suitable diplexers. Microwave complementary component filters are shown to fulfill the requirement for the design of diplexing and multichannel filters with theoretically perfect match at all frequencies.

A design procedure using component networks with Chebyshev characteristics is given. This allows a narrow crossover region and high isolation to be obtained for a given network complexity at the cost of a slight increase in input-port VSWR (Voltage Standing-Wave Ratio). The design procedure makes use of published tables and does not require a detailed knowledge of synthesis techniques.

Experimental results for two diplexing networks, one a complementary pair and the other a Chebyshev pair, are given in verification of the theory presented.

I. INTRODUCTION

THE DESIGN of passive multichannel filters requires a network that will separate a given frequency band into N channels with minimum insertion loss and low-input-port VSWR. The complexity of the network is determined by the allowable width of contiguous channel crossover regions and the required isolation between bands.

The design approach reported in this paper uses a number of two-channel filters (diplexers) as basic building blocks in obtaining the N -channel filter as shown in Fig. 1. A design technique for multiplexers using a different network configuration is given in Cristal and Matthaei [1]. By using exact synthesis techniques, a three-port network with the desired band separation and a low-input VSWR over a broad frequency range is obtained. Networks of this type can then be used, in cascade, to realize multichannel filters.

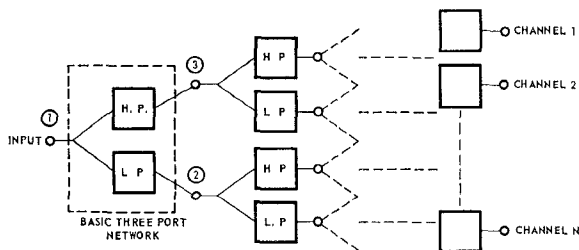


Fig. 1. General configuration of N -channel filter.

II. THE "IDEAL" DIPLEXER

An "ideal" diplexer is defined as a lossless, resistively terminated three-port network that separates the frequency spectrum into two isolated bands with a perfect match at the input port.

The network to be considered for the ideal diplexer is that of two parallel-connected, resistively terminated, lossless filters, one of which is low-pass, and the other high-pass¹ as indicated schematically in Fig. 2.

A simple parallel connection of low-pass and high-pass filters does not insure that the resulting network will approximate the ideal diplexer characteristic. In most single-filter design procedures, only the transmission response is considered and little attention is given to the input admittance characteristics. In the stop-band, the input admittance of the filter will be a susceptance that varies with frequency, and thus, one that will seriously affect the performance of another filter connected in parallel. For narrow-band channels separated by guard bands, a good match only may be required over the narrow pass-bands involved, and conventional design procedures can be employed [3]. Where the bandwidths involved are moderate to wide and the channels are contiguous, special techniques are required.

A parallel connection of networks of the type shown in Fig. 2 provides a perfect match at the input port if the component filters are defined as complementary.² This requires that the input admittances of the low-pass and of the high-pass filters obey the normalized relationship

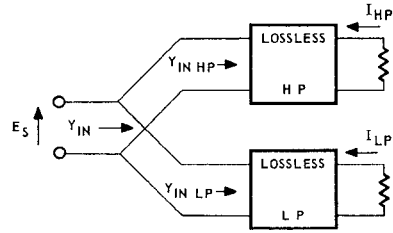
$$Y_{in} = Y_{inLP} + Y_{inHP} = 1. \quad (1)$$

Consequently, the sum of real parts of the input admittances must be constant and the reactive parts must be equal and of opposite sign. Thus

$$\begin{aligned} \operatorname{Re} [Y_{inLP}] + \operatorname{Re} [Y_{inHP}] &= 1 \\ \operatorname{Im} [Y_{inLP}] + \operatorname{Im} [Y_{inHP}] &= 0. \end{aligned} \quad (2)$$

¹ The analysis for the dual case of series-connected networks follows in an analogous manner. The admittance case is, in general, more applicable for implementation at microwave frequencies. Because of the repetitive nature of the microwave networks to be considered, the high-pass filter becomes a band-pass filter, and the low-pass filter becomes a stop-band filter [2]. Thus, only low-pass and high-pass characteristics need be investigated.

² A thorough discussion of complementary filters can be found in Guillemin [4] and Weinberg [5]. Examples of microwave components are given by Wenzel [2].



$$Y_{IN} = Y_{IN LP} + Y_{IN HP} = \text{Re} [Y_{IN LP}] + j \text{Im} [Y_{IN LP}] + \text{Re} [Y_{IN HP}] + j \text{Im} [Y_{IN HP}]$$

$$|Y_{12}|_{HP}^2 = \left| \frac{I_{HP}}{E_s} \right|^2$$

$$|Y_{12}|_{LP}^2 = \left| \frac{I_{LP}}{E_s} \right|^2$$

Fig. 2. Basic diplexer configuration and network definitions.

For lossless networks terminated in a unit resistance

$$\text{Re} [Y_{in}] = |Y_{12}|^2 \quad (3)$$

where Y_{12} is the ratio of output current to input voltage. (See Guillemin [4], p. 446.) Therefore, (1), (2), and (3) require that

$$|Y_{12}|_{LP}^2 + |Y_{12}|_{HP}^2 = 1. \quad (4)$$

To design a complementary filter pair, it is necessary to designate the $|Y_{12}|^2$ in (4) with suitable functions and then to synthesize networks that realize these functions. Details of methods used in function designation, sometimes referred to as the "approximation problem," can be found in Guillemin [4] and Weinberg [5]. In most instances, this lengthy process can be avoided by the use of tables [5], [6]. To obtain low-input VSWR at all frequencies, it is necessary that the input admittances of the component filters be realized exactly. Exact synthesis procedures for microwave TEM-mode networks consisting of quarter-wave lines can be found in Ozaki and Ishii [7], [8], Grayzel [9], Shiffman and Matthaei [10], and also in Wenzel [2]. The microwave networks can be designed by applying lumped element techniques, and using the transformation

$$S = j\Omega = j \tan \frac{\pi\omega}{2\omega_0}.$$

A straightforward application of Kuroda's identities [2], [8] and/or Richard's theorem [11] then leads to practical microwave structures with characteristics that are known theoretically at all frequencies.

Complementary filter design, based on transfer admittance prototype networks, requires the use of singly terminated networks rather than the doubly terminated networks more commonly used at microwave frequencies. Thus, each component network is designed as though it were being driven by an ideal voltage source rather than with a matched generator. When the two complementary networks are connected in parallel, the input admittance becomes purely conductive. Thus, if

the network is driven by a matched source, the input voltage remains constant as was assumed in the design of the component filters. The characteristics of the network pairs are determined by both the magnitude and phase of the input admittance rather than by a magnitude function alone as in conventional, doubly terminated microwave filter design. To achieve the desired performance, techniques must be used that preserve both the magnitude and phase characteristics of the input admittance. Exact synthesis procedures are ideally suited to meeting these requirements.

A commonly used low-pass filter characteristic, suitable for use in designing a complementary filter pair is the n th order Butterworth function given by

$$|Y_{12}|_{LP}^2 = \frac{1}{1 + \Omega^{2n}} \quad (5)$$

where

$$\Omega = \tan \frac{\pi\omega}{2\omega_0}.$$

The complementary characteristic is given by

$$|Y_{12}|_{HP}^2 = \frac{\Omega^{2n}}{1 + \Omega^{2n}}. \quad (6)$$

The element values in the ladder prototype for the low-pass filter can be obtained from tables [5], [6]. The high-pass network has the same geometry as that of the low-pass network with every element being replaced by its dual and having a reciprocal element value [2].

Prototype networks for the third-order filter pair are shown in Fig. 3(a).³ To obtain a realizable microwave structure, unit elements of characteristic im-

³ The capacitor and inductor symbols in Fig. 3 are used to represent open-circuited and short-circuited quarter-wave sections of transmission line, respectively [2], [12].

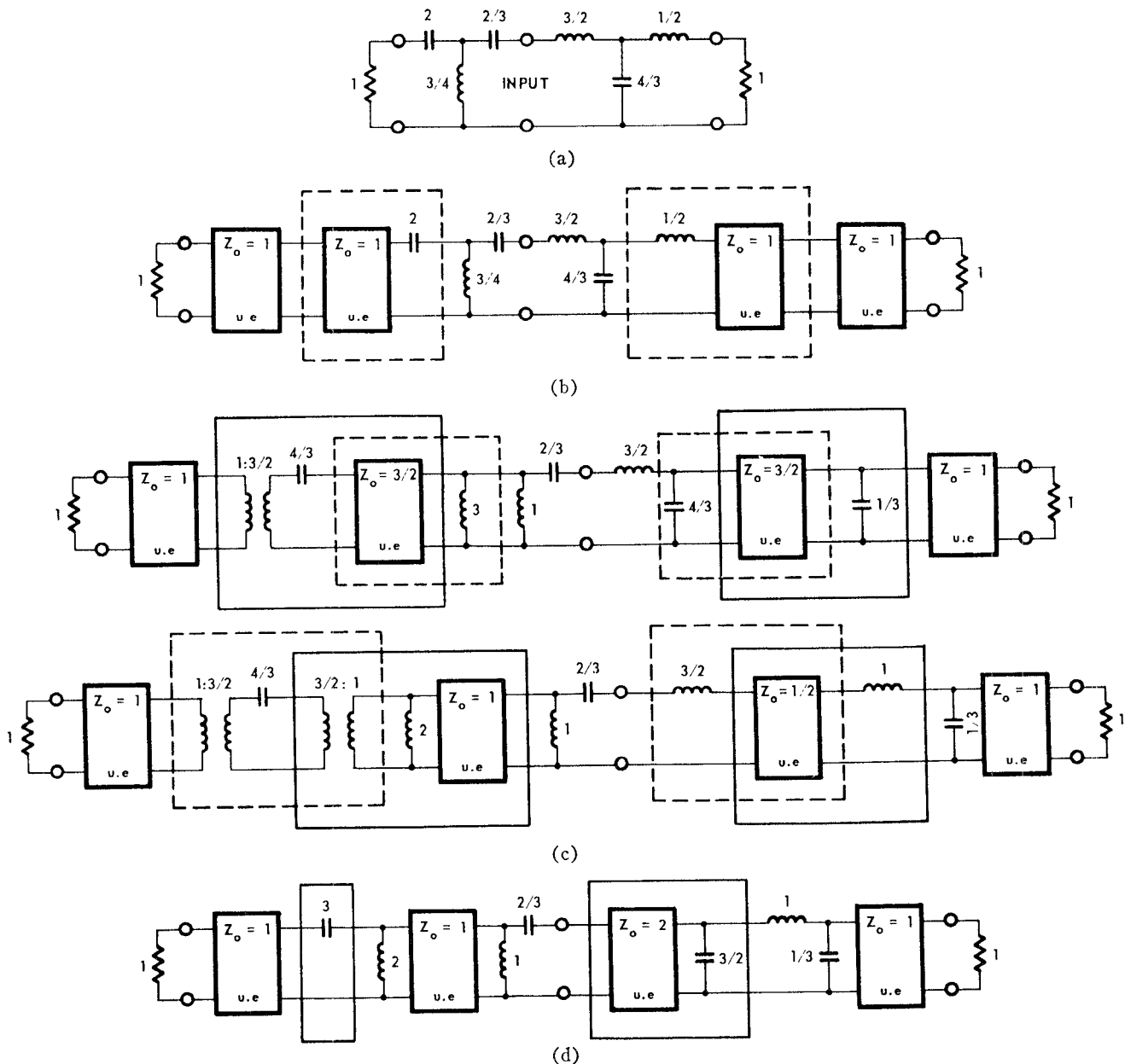


Fig. 3. (a) Third-order butterworth complementary filter pair prototype. (b) Insertion of unit elements ($\mu.e.$). Note: The dotted lines indicate the section that will be transformed in the next diagram. The solid lines indicate the results of the previous transformation. (c) Application of Kuroda's identities. (d) Final circuit.

pedance $Z_0=1$ are inserted between each network and its load as shown in Fig. 3(b). This changes the phase of the transfer admittances, but maintains the input admittance unchanged. Kuroda's identities now can be applied to obtain a practical realization. One method of accomplishing this is demonstrated in Fig. 3(c). As is evident, the physical form of the filter pairs is not unique. The identities can be further applied to the final circuit, Fig. 3(d), and many other realizations can be obtained. The manner in which the identities are applied is dictated by the practical realizability of resulting element values. For the series capacitors and shunt inductors, care must be taken in applying the transformations so that ideal transformers are not generated. In the foregoing example, this is accomplished

by splitting the shunt inductor in Fig. 3(c) in such a way that the resulting transformer has the same turns ratio, but of opposite sense, as that generated by the series capacitor transformation [2].

A practical microwave realization⁴ of the above diplexer is shown in Fig. 4 and an experimental model is shown in Fig. 5. The experimental input VSWR and transfer characteristics in the frequency range 0 to 8 Gc/s are given in Fig. 6. The repetitive nature of the distributed lines results in multiple crossover points. If only one crossover is of interest—as is often the case—maximum experimental VSWRs of less than 1.2 are easily

⁴ The manner in which the numbers associated with the prototype are converted to transmission line dimensions is discussed thoroughly in [2], [7], [9], and [12].

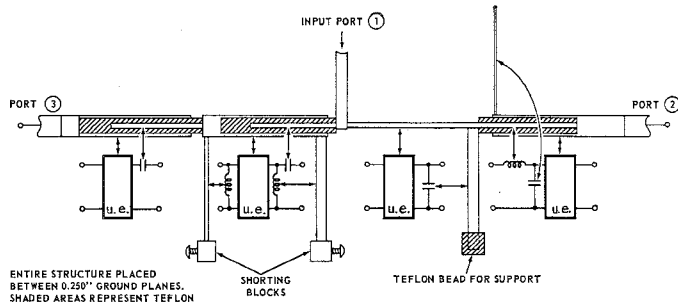


Fig. 4. Diagram of TEM circuit that realizes a third-order Butterworth complementary filter pair.

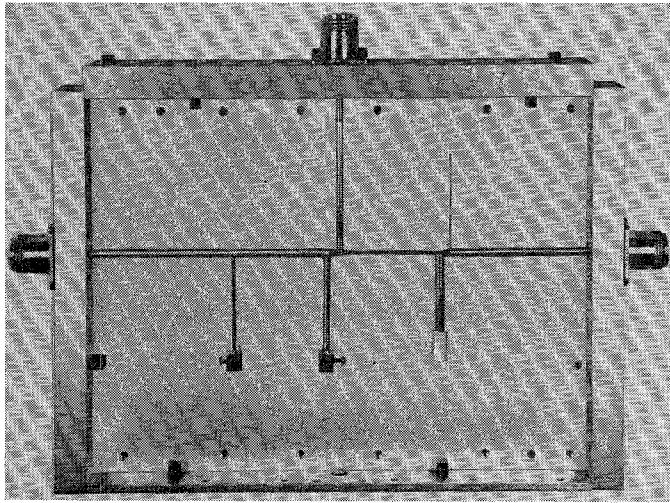


Fig. 5. Third-order Butterworth complementary filters.

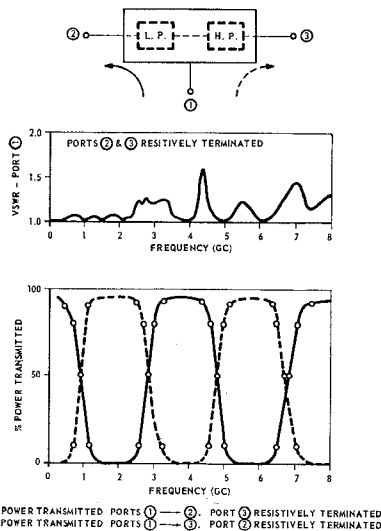


Fig. 6. Measured insertion loss and VSWR characteristics of third-order Butterworth complementary filters.

obtainable. Sharper crossover characteristics can be obtained by using filters of a higher order. Any desirable bandwidth can be obtained by frequency scaling the prototype networks [2].

The above diplexer is "ideal" in the sense that it has an input match that is theoretically perfect. It is "non-ideal" in that only for an infinite number of filter elements does the crossover region become zero in width. Steeper filter skirts, and consequently a narrower crossover region, can be obtained for a given number of filter elements if a Chebyshev approximation to the desired characteristic is employed. From the viewpoint of input VSWR, the optimum condition occurs when the filters are complementary. However, imposing this condition on Chebyshev filter pairs leads to poor isolation. This effect can be understood by considering a 0.1 dB ripple filter. When the power response of this filter is down 0.1 dB or approximately two per cent, the response of a true complement must pass the two per cent power resulting in only 17 dB isolation. However, this amount of isolation is insufficient in many practical situations. Thus, requiring the input VSWR to be 1.0 puts a severe restriction on the width of the crossover region and the realizable isolation. Intuitively, one expects that it should be possible to improve the isolation and crossover characteristics by relaxing the input VSWR requirement.

III. NARROWER CROSSOVER REGIONS OBTAINED BY INPUT-PORT MISMATCH

Insight into the manner in which the VSWR requirement might be relaxed can be obtained by considering the mathematical form of the pertinent filter characteristics. A significant fact is that the input admittances associated with parallel-connected complementary filters are minimum susceptible, i.e., they do not contain j -axis poles. Under this condition, the admittances are analytic in a one-half plane and have real and imaginary parts that are Hilbert transforms. Thus

$$\text{Im} [Y_{in}(\Omega)] = -\frac{1}{\pi} \int_{-\infty}^{+\infty} \frac{\text{Re} [Y_{in}(x)] dx}{\Omega - x} \quad (7)$$

For the functions under consideration, one can differentiate both real and imaginary parts of Y_{in} a number of times, carry out the indicated integration, and then integrate the left-hand side the same number of times it had been originally differentiated to obtain $\text{Im} [Y_{in}(\Omega)]$. That is

$$\left. \begin{aligned} \frac{d^n \text{Im} [Y_{in}(\Omega)]}{d\Omega^n} &= -\frac{1}{\pi} \int_{-\infty}^{+\infty} \frac{\frac{d^n \text{Re} [Y_{in}(x)]}{dx^n}}{\Omega - x} dx \\ &= -\frac{1}{\pi} \int_{-\infty}^{+\infty} \frac{d^n [|Y_{12}(x)|_{LP}^2 + |Y_{12}(x)|_{HP}^2]}{dx^n} dx \end{aligned} \right\} \quad (8)$$

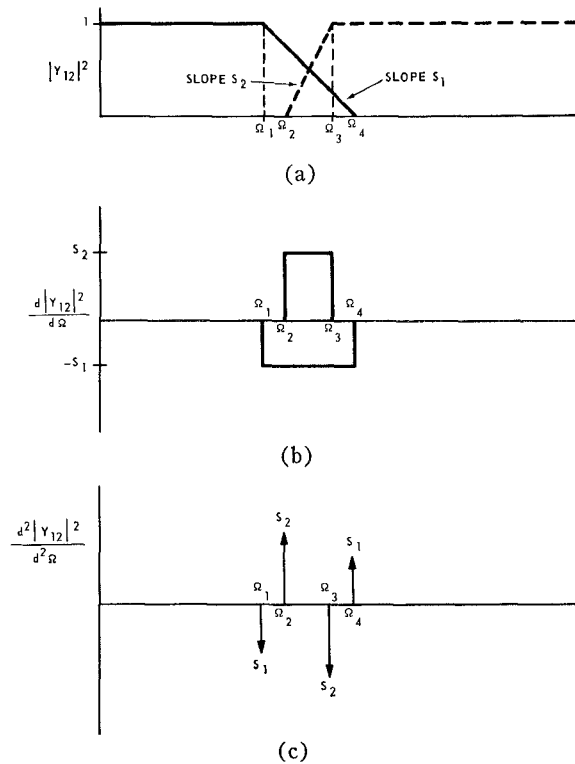


Fig. 7.—(a) Piecewise linear low-pass high-pass filter characteristics $|Y_{12}|^2 = \text{Re}(Y_{in}^0)$. (b) First derivative of filter characteristics. (c) Second derivative of filter characteristics.

Equation (8) provides a convenient method of calculating—numerically and graphically—the input VSWR of a filter pair and demonstrates the factors which most influence the obtainable characteristics.⁵ Using criteria derived from this relation, it is possible to build filter pairs with low-input VSWR and crossover characteristics that are significantly better than the Butterworth characteristics of comparable order. These filters are synthesized with the use of an exact theory, and thus have characteristics that can be specified theoretically at all frequencies.

As an example of applying the above relation, consider the piecewise linear, low-pass high-pass filter pair characteristics shown in Fig. 7(a). First and second derivatives of the characteristics are shown, respectively, in Fig. 7(b) and 7(c). Since the second derivative functions have been reduced to a set of impulses, the integral in (8) can be evaluated by inspection and the imaginary part can be determined by two integrations of the resulting function. A good design criterion can be obtained from Fig. 7(c). Location of the impulses is determined by the filter break points, and their magnitudes are determined by the slope of the filter characteristics. Thus, if the break points are forced to occur at the same frequencies and the slopes of the filter characteristics are made equal and opposite, the impulses will cancel, and result in a zero imaginary part. Under these

conditions, the real parts must add to unity as in the case of true complements.

Computations similar to the above example show that any filter pair that has an input admittance with a real part of approximately unity at all frequencies, and that is devoid of extremely rapid variations in its characteristic will have an imaginary part that is quite small and will exhibit good diplexing properties. Therefore, any low-pass high-pass filter pair for which $|Y_{12}|^2_{\text{LP}} + |Y_{12}|^2_{\text{HP}} \approx 1$ will be suitable.

One method of obtaining input admittances that add to approximately unity is to set the 3 dB points of the filter characteristics equal to each other, and to set the slope of the high-pass filter equal to the negative of the low-pass slope at the 3 dB point. As a starting point, a low-pass Chebyshev prototype network is chosen where

$$|Y_{12}(\Omega)|^2_{\text{LP}} = \frac{1}{1 + \epsilon^2 T_n^2(\Omega)} \quad (9)$$

This function has a pass-band ripple determined by ϵ and is monotonic in the stop-band. For reasons previously discussed, the true complement should not be used for the high-pass network. A suitable functional characteristic can be obtained by applying the low-pass to high-pass transformation (by substituting $1/\Omega$ for Ω) to (9) giving

$$|Y_{12}(\Omega)|^2_{\text{HP}} = \frac{1}{1 + \epsilon^2 T_n^2\left(\frac{1}{\Omega}\right)} \quad (10)$$

⁵ For examples of numerical calculations see Guillemin [4], pp. 296–308.

This characteristic has a monotonic stop-band, and pass-band ripple determined by ϵ . It does not provide the desired characteristic in that it "crosses over" the chosen low-pass function of (9) at $\Omega=1$, or at the specified ripple value rather than the 3 dB point. This problem can be eliminated by frequency scaling the high-pass network which is accomplished by substituting Ω/k for Ω in (10). The 3 dB frequency for the low-pass filter [13] is given by

$$\Omega_{3\text{ dB}} = \cosh \left[\frac{\cosh^{-1} \left(\frac{1}{\epsilon} \right)}{n} \right] \quad (11)$$

where n is the number of filter sections. Therefore, k is given by solution of

$$T_n^2(\Omega_{3\text{ dB}}) = T_n^2 \left(\frac{k}{\Omega_{3\text{ dB}}} \right) \quad (12)$$

or

$$k = \Omega_{3\text{ dB}}^2 = \cosh^2 \left[\frac{\cosh^{-1} \left(\frac{1}{\epsilon} \right)}{n} \right]. \quad (13)$$

Thus, the requirement that the 3 dB points for each characteristic occur at the same frequency has been satisfied.

The second requirement, that the characteristics have slopes that are equal and opposite at the 3 dB frequency, is also satisfied by the above transformation and renormalization as shown in the Appendix. The desired network characteristics thus are given by

$$|Y_{12}|_{\text{LP}}^2 = \frac{1}{1 + \epsilon^2 T_n^2(\Omega)} \quad (14)$$

and

$$|Y_{12}|_{\text{HP}}^2 = \frac{1}{1 + \epsilon^2 T_n^2 \left(\frac{k}{\Omega} \right)}.$$

An important aspect of the above procedure is that networks with quite high ripples (on the order of 1 dB) in their $|Y_{12}|^2$ functions, with consequent steep band-edge skirts, can be used without obtaining significant ripple in insertion loss. Thus, one obtains the advantage of skirt selectivity associated with a high-ripple filter together with the pass-band insertion loss characteristic of a low-ripple filter. At first thought, this result may appear to contradict the known optimum responses obtainable using a given number of filter elements. For example, it is known that a low-pass filter containing N elements has an established optimum response in

terms of skirt slope and pass-band ripple. An improvement over this optimum response for the diplexing network containing two N -element networks is possible since the high-pass filter stop-band input admittance aids the pass-band response of the low-pass filter, and vice versa. In effect, the pass-band insertion loss response of each filter in the pair is determined by two N -element filters and thus can provide a response better than the optimum for an N -element filter.

The fact that low-pass-band ripple can be obtained from a filter pair having large ripple in its transfer admittance characteristics also can be seen by considering the input admittance of each filter in the pair. Since $\text{Re}[Y_{\text{in}}] = |Y_{12}|^2$, each filter has an input admittance whose real part exhibits relatively large ripples. If the real parts add to approximately unity (within 20 per cent, for example) and do not vary rapidly, the imaginary parts will be approximately equal and opposite and will tend to cancel. Under these conditions, the component networks appear as two conductances in parallel, one that varies as $|Y_{12}|_{\text{LP}}^2$ and the other as $|Y_{12}|_{\text{HP}}^2$. Ripple in the $|Y_{12}|^2$ functions thus is presented at the input port as a resistive ripple. A $|Y_{12}|^2$ ripple of 1 dB corresponds to a resistive variation of approximately 1.25 to 1 and, therefore, to an input VSWR variation of 1.25 to 1. This results in a very small transmission ripple. In general, for ripple values for 1 dB or less, the maximum input VSWR is approximately $\text{antilog}_{10}(\alpha/10)$, where α is the ripple in dB. In practice, the input VSWR is slightly higher than this value since the input susceptance is not exactly zero.

Element values for the network that realizes the low-pass characteristic of (14) can be obtained from tables in Weinberg [5], [6]. The high-pass network is obtained by inspection using a procedure similar to that for the Butterworth networks. The low-pass to high-pass transformation results in a high-pass network having the same geometry as the low-pass network with every element having been replaced by its dual with a reciprocal value. Frequency scaling by the factor

$$k = \cosh^2 \left[\frac{\cosh^{-1} \left(\frac{1}{\epsilon} \right)}{n} \right]$$

is then accomplished by dividing all of the element values in the high-pass network by k .

The following design example demonstrates the technique described above. For simplicity, a two-section design will be described. Extension to higher order filter pairs follows in a straightforward manner.

The design procedure is initiated by choosing the low-pass filter which, in the present example, is a two-section 1-dB ripple Chebyshev transfer admittance prototype shown in Fig. 8(a) (page 12). The low-pass to high-pass transformation gives the network of Fig. 8(b).

For a 1-dB ripple, $\epsilon = 0.51$; therefore, from (13), $k = 1.48$. Dividing the element values of the network of Fig. 8(b) by k gives the final prototype shown in Fig. 8(c). To complete the design, unit elements are inserted adjacent to the load as for the Butterworth example and Kuroda's identities are applied. Because of the simple nature of each filter, both can be built without actually applying Kuroda's identities. The introduction of a one-unit element before each load is sufficient. However, this requires that the shunt inductor and capacitor be placed on opposite sides of the line to insure that there is no interaction between their fields. The input port then has to be connected at right angles to the plane of the filter structure. This can be a suitable configuration at low frequencies but might easily lead to radiation in C band or X band. To alleviate this problem, the high-pass prototype was left in its original form and Kuroda's identities were applied to the low-pass structure to move the capacitor away from the filter junction. One application of Kuroda's identity yields the circuit of Fig. 8(d). In order to make the construction simple, the input inductor was separated into a series connection of two inductors, and Kuroda's identity was applied to yield a design in which all the unit elements had a value equal to the characteristic impedance of the system, and all the stub impedances were easily realizable. The final prototype network is shown in Fig. 8(e). A diagram of an experimental circuit that realizes the network of Fig. 8(e) is shown in Fig. 9(a). The performance of the filter pair can be obtained by direct analysis. Referring to Fig. 8(c), the normalized output powers are $4|V_3(j\Omega)|^2$ and $4|V_2(j\Omega)|^2$ for the low-pass and high-pass channels, respectively. Both theoretical and experimental power transmission curves as well as input VSWR are shown in Fig. 9(b).

The computed characteristics of a five-section 1-dB ripple Chebyshev transfer admittance characteristic are shown in Fig. 10. The improvement in crossover width relative to that of a Butterworth characteristic of the same order is significant. The cost is only a small increase in input VSWR.

IV. MULTICHANNEL FILTERS

The exact design procedure for the diplexer now may be extended to handle contiguous multiple channels. The theoretically perfect match of each diplexer can be maintained at the input of the N -channel filter by using complementary filter pairs. If a slight input-port mismatch can be tolerated, Chebyshev filter characteristics can be used resulting in a decrease in network complexity for a given crossover width and isolation requirement. As an example, assume that it is desired to separate the frequency band 1 to 12 Gc/s into four bands—1 to 2, 2 to 4, 4 to 8, and 8 to 12 Gc/s, respectively. One method of accomplishing this separation is indicated in Fig. 11(a). The first diplexer has a cross-

over at 4 Gc/s and is constructed of transmission lines having a quarter-wavelength at a frequency, f_0 , of 8 Gc/s. The resulting 1 to 4 Gc/s and 4 to 12 Gc/s bands are then split by the use of two more diplexing networks.

An alternate method that uses the repeating nature of the exactly designed networks is shown in Fig. 11(b). The first diplexer is constructed about a center frequency of 6 Gc/s and divides the 1 to 12 Gc/s band into three bands: 1 to 4, 8 to 12, and 4 to 8 Gc/s. The 1 to 4 Gc/s and 8 to 12 Gc/s bands are widely separated, and can be split with a relatively simple diplexer (three sections may be adequate). The 1 to 4 Gc/s band is then split as in the first method.

The second approach to multiplexing the contiguous bands in the above example has distinct advantages over the first. Only two of the component diplexers need have narrow crossover regions. Furthermore, the 1 to 12 Gc/s diplexer which, in general, might be the most difficult to construct because it must work over a very wide band, now is constructed by using 6 Gc/s quarter-wave elements rather than 8 Gc/s elements and, therefore, is less susceptible to undesirable junction effects.

V. ALTERNATE FORMS OF COMPLEMENTARY PAIRS

The diplexing networks discussed so far have had $L-C^6$ ladder prototypes, and have led to physical realizations of the type shown in Fig. 4 and 9(a). Use can be made of a number of circuit equivalents [2] to obtain different practical realizations. Another important class of microwave filters are those that do not have a prototype of this form. These include:

- 1) Parallel coupled bars with open ends
- 2) Parallel coupled bars with shorted ends
- 3) Uniform line with quarter-wave spaced series open stubs
- 4) Uniform line with quarter-wave spaced shunt-shortened stubs
- 5) Stepped quarter-wave sections with one series open stub
- 6) Stepped quarter-wave sections with one shunt-shortened stub

Diplexers also can be designed in these forms using the same methods outlined in Sections II and III. An exact synthesis procedure for networks of this type is given by Wenzel [2]. Because these networks have but a single pole in their transfer response, they are most useful in relatively narrow-band designs. The existence of only one singularity degrades the realizable skirt characteristics for wide bandwidths. On the other hand, for narrow-band designs, the networks are often easier to construct in this form.

⁶ Again, the use of the symbols L and C are taken to mean the short-circuited and open-circuited distributed quarter-wave line, respectively.

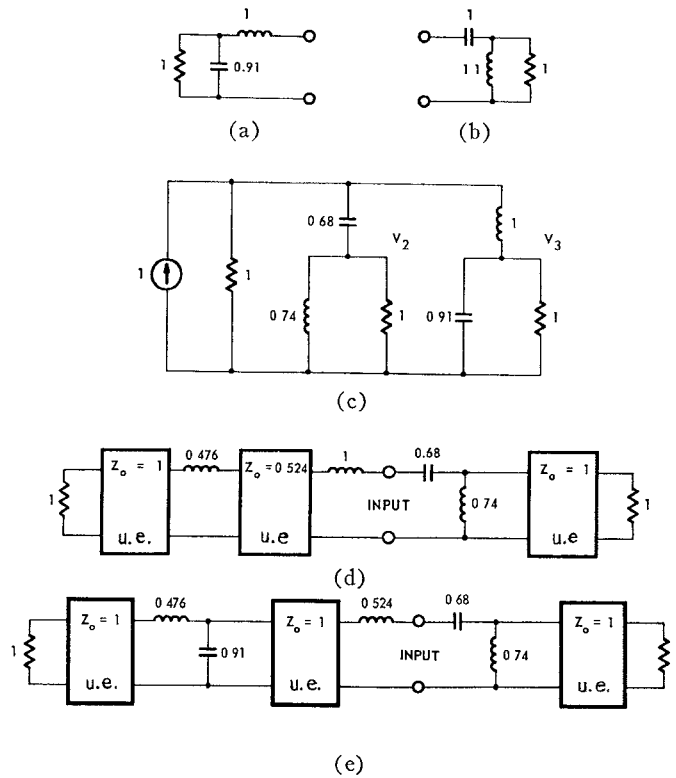


Fig. 8.—(a) Low-pass 1-dB ripple $|Y_{12}|^2$ prototype. (b) High-pass filter prototype. (c) Final prototype circuits from which performance characteristics can be obtained by direct analysis. (d) Prototype after one application of Kuroda's identity. (e) Practical prototype after insertion of unit elements and application of Kuroda's identities.

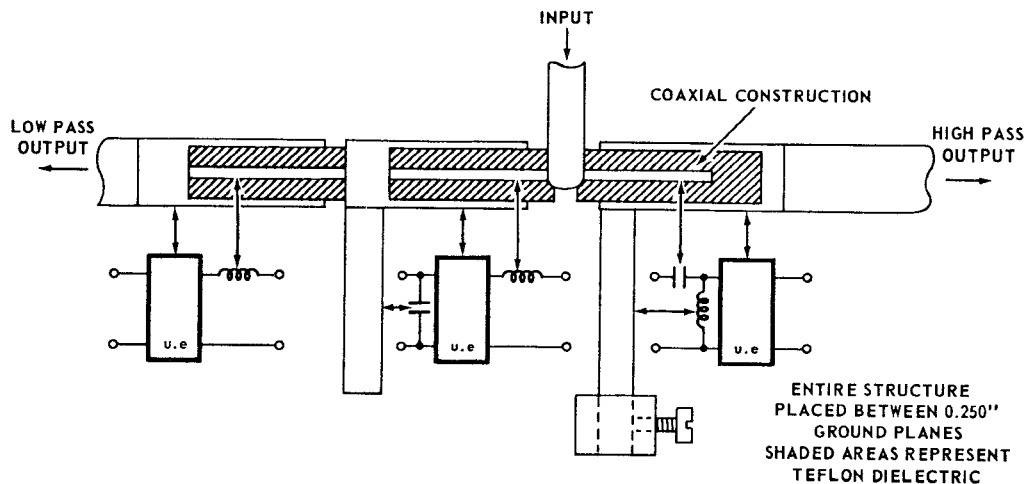


Fig. 9. (a) Experimental circuit that realizes a two-section 1-dB ripple Chebyshev filter pair. (*cont'd.*)

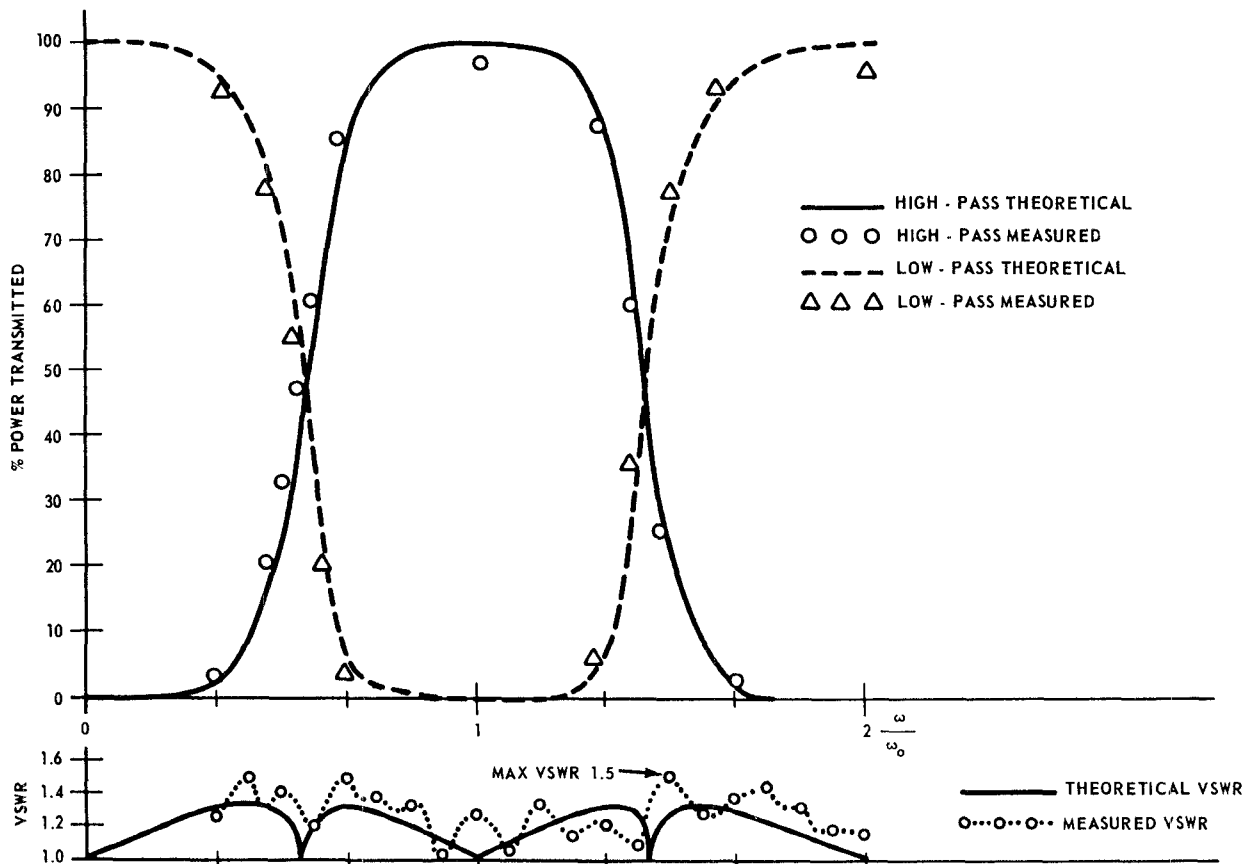


Fig. 9 (b) Theoretical and experiment characteristics of the filter pair.

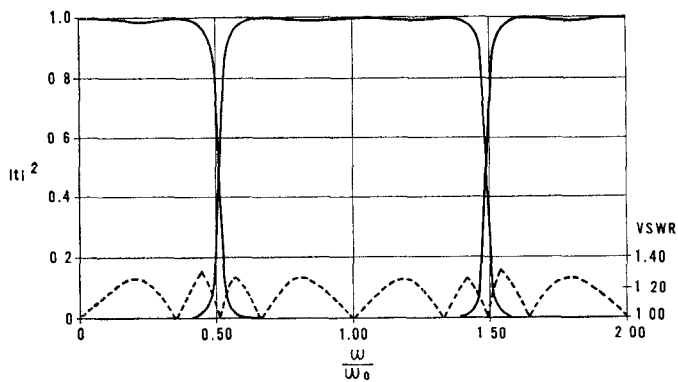


Fig. 10.—Computed characteristics of a five-section filter pair that uses 1-dB ripple transfer admittance prototypes.

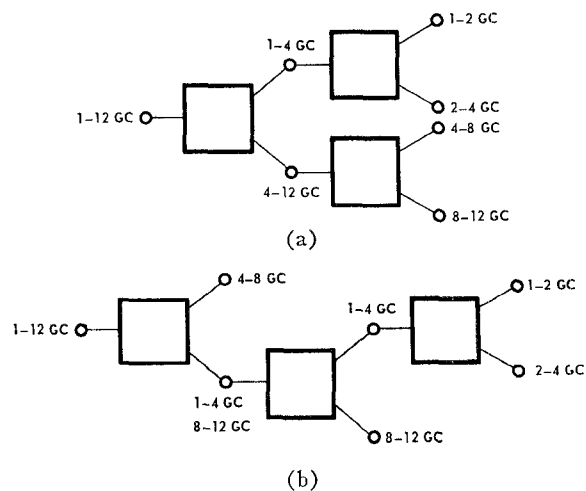


Fig. 11—Wide-band multichannel filters. (a) Network requiring narrow crossover characteristics for each diplexer. (b) Network requiring only two diplexers with narrow crossover regions.

VI. CONCLUSIONS

Microwave complementary component filters, based on exact design procedures, have been shown to fulfill the requirement for the design of diplexing and multi-channel filters with theoretically perfect match at all frequencies. By allowing the input to be slightly mismatched, steeper skirt characteristics, and consequently, narrower crossover regions, can be obtained for a given number of sections. In general, there are five factors of major importance in a multiplexing network—input VSWR, crossover width, isolation, loss, and network complexity. An optimum network might be defined in different ways depending on which of these five factors is of most importance. If an extremely good input match is required, the filters should be made complementary. Losses in multichannel filters of this type will tend to be minimal due to the good match and absence of internal reflections. If slight input-port mismatch can be tolerated, use of Chebyshev characteristics provides better isolation and narrower crossover width for a given filter complexity. In multichannel applications requiring a large number of cascaded filter pairs, the use of Chebyshev characteristics with large ripple values may result in a high overall input VSWR due to an accumulation of the relatively small VSWRs of each component filter pair. The overall loss of a structure of this type will increase due to the input mismatch and dissipation loss caused by internal reflections. The designer must consider which of the performance factors are of greatest importance, and then must select the network characteristics to obtain the best results.

The procedure given for designing networks with input mismatch leads to networks with good performance characteristics and, in general, is quite simple to apply. In verification of the theory presented, the measured performance of two experimental diplexing networks closely followed the predicted performance over an extremely wide frequency range. The computed characteristics of a five-section filter pair designed from 1-dB ripple Chebyshev transfer admittance prototypes demonstrated that, for moderate ripple values, the resulting maximum input VSWR is approximately that which would be caused by a resistive mismatch of $\text{antilog}_{10}(\alpha/10)$, where α is the prototype ripple in dB.

APPENDIX

Given the characteristics

$$\left| Y_{12}(\Omega) \right|_{\text{LP}}^2 = \frac{1}{1 + \epsilon^2 T_n^2(\Omega)} \quad (1)$$

and

$$\left| Y_{12}(\Omega) \right|_{\text{HP}}^2 = \frac{1}{1 + \epsilon^2 T_n^2\left(\frac{k}{\Omega}\right)}$$

where

$$k = (\Omega_{3 \text{ dB}})^2 = \cosh^2 \left[\frac{\cosh^{-1}\left(\frac{1}{\epsilon}\right)}{n} \right] \quad (2)$$

and n = the number of filter sections, then

$$\left. \frac{d \left| Y_{12}(\Omega) \right|_{\text{LP}}^2}{d\Omega} \right|_{\Omega_{3 \text{ dB}}} = \left. \frac{-2\epsilon^2 T_n(\Omega) \frac{d}{d\Omega} T_n(\Omega)}{[1 + \epsilon^2 T_n^2(\Omega)]^2} \right|_{\Omega_{3 \text{ dB}}} \quad (3)$$

and

$$\left. \frac{d \left| Y_{12}(\Omega) \right|_{\text{HP}}^2}{d\Omega} \right|_{\Omega_{3 \text{ dB}}} = \left. \frac{-2\epsilon^2 T_n\left(\frac{k}{\Omega}\right) \frac{d}{d\Omega} T_n\left(\frac{k}{\Omega}\right)}{\left[1 + \epsilon^2 T_n^2\left(\frac{k}{\Omega}\right)\right]^2} \right|_{\Omega_{3 \text{ dB}}}$$

Use of (2) shows that the only factors that need be considered are

$$T_n(\Omega) \frac{d}{d\Omega} T_n(\Omega) \Big|_{\Omega_{3 \text{ dB}}} \quad (4)$$

and

$$T_n\left(\frac{k}{\Omega}\right) \frac{d}{d\Omega} T_n\left(\frac{k}{\Omega}\right) \Big|_{\Omega_{3 \text{ dB}}}$$

Now

$$T_n(X) = \cos(n \cos^{-1} X).$$

Therefore,

$$T_n(\Omega) \frac{d}{d\Omega} T_n(\Omega) \Big|_{\Omega_{3 \text{ dB}}} = \frac{n T_n(\Omega) \sin(n \cos^{-1} \Omega)}{[1 - \Omega^2]^{1/2}} \Big|_{\Omega_{3 \text{ dB}}} \quad (5)$$

and

$$\begin{aligned} T_n\left(\frac{k}{\Omega}\right) \frac{d}{d\Omega} T_n\left(\frac{k}{\Omega}\right) \Big|_{\Omega_{3 \text{ dB}}} \\ = \frac{-nk T_n\left(\frac{k}{\Omega}\right) \sin\left(n \cos^{-1} \frac{k}{\Omega}\right)}{\Omega^2 [1 - \Omega^2]^{1/2}} \Big|_{\Omega_{3 \text{ dB}}} \end{aligned}$$

Substitution of (2) shows the slopes to be equal and opposite.

ACKNOWLEDGMENT

The author is indebted to M. C. Horton for proof-reading the original manuscript and for his many helpful comments and suggestions. Appreciation is also expressed for discussions with P. C. Goodman which were very helpful in formulating the approach taken; to A. Gianetti and T. Gordon for their work in constructing the experimental diplexers.

REFERENCES

- [1] Cristal, E. G., and G. L. Matthaei, A technique for the design of multiplexers having contiguous channels, *IEEE Trans. on Microwave Theory and Techniques*, vol MTT-12, Jan 1964, pp 88-93.
- [2] Wenzel, R. J., Exact design of TEM microwave network using quarter-wave lines, *ibid*, pp 94-111.
- [3] Ragan, G. L., *Microwave Transmission Circuits*, MIT Rad Lab Series, New York: McGraw-Hill, vol 9, 1948, pp 708-9.
- [4] Guillemin, E. A., *Synthesis of Passive Networks*, New York: John Wiley, 1957.
- [5] Weinberg, L., *Network Analysis and Synthesis*, New York: McGraw-Hill, 1962.
- [6] Weinberg, L., Network design by use of modern synthesis techniques and tables, *Proc. NEC*, vol 12, 1956, pp 704-817.
- [7] Ozaki, H., and J. Ishii, Synthesis of transmission-line networks and the design of UHF filters, *IRE Trans. on Circuit Theory*, vol CT-3, Dec 1956, pp 325-336.
- [8] Ozaki, H., and J. Ishii, Synthesis of a class of strip-line filters, *IRE Trans. on Circuit Theory*, vol CT-5, Jun 1958, pp 104-109.
- [9] Grayzel, A. I., A synthesis procedure for transmission-line networks, *IRE Trans. on Circuit Theory*, vol CT-5, Sep 1958, pp 172-181.
- [10] Schiffman, B. M., and G. L. Matthaei, Exact design of band-stop microwave filters, *IEEE Trans. on Microwave Theory and Techniques*, vol MTT-12, Jan 1964, pp 6-15.
- [11] Richards, P. I., Resistor transmission-line circuits, *Proc. IRE*, vol 36, Feb 1948, pp 217-220.
- [12] Horton, M. C., and R. J. Wenzel, Distributed filter design using exact techniques, *Microwaves*, Apr 1964, pp 16-21.
- [13] Mager, H., The Chebyshev normalized low-pass 3 dB frequency—a bone from the technical graveyard? *IEEE Trans. on Circuit Theory (Correspondence)*, vol CT-10, Jun 1963, pp 287-288.

Operation of the Ferrite Junction Circulator

C. E. FAY FELLOW, IEEE, AND R. L. COMSTOCK MEMBER, IEEE

Abstract—The operation of symmetrical circulators is described in terms of the counter-rotating normal modes (fields varying as $\exp n\phi$) of the ferrite-loaded circuits. The rotating modes, which are split by the applied magnetic field, form a stationary pattern which can be rotated in space to isolate one of the ports of the circulator. A detailed field theory of the strip-line Y -junction circulator operating with $n=1$ is presented. Experiments designed to confirm the validity of the rotating normal mode description of circulator action in the Y -junction circulator also are presented; these include measurements of mode frequencies and electric field patterns. The results of the field theory are used in a design procedure for quarter-wave coupled strip-line circulators. The results of the design procedure are shown to compare adequately with experimental circulators. Higher mode operation of strip-line circulators is described. The operation of waveguide cavity circulators is shown to depend on the rotating ferrite-loaded cavity modes.

INTRODUCTION

A VERSATILE MICROWAVE DEVICE which is becoming one of the most widely used is the ferrite junction circulator. Its versatility is indicated by the fact that in addition to its use as a circulator, it also can be used as an isolator or as a switch. The three-port version of the ferrite junction circulator, usually called the Y -junction circulator, is most commonly used. It can be constructed in either rectangular waveguide or strip line. The waveguide version is usually an H -plane junction, although E -plane junction circulators also can be made. The strip-line ferrite junction circulator is usually made with coaxial connectors and is principally applicable to the UHF and low-microwave frequencies.

The ferrite junction circulator was in use for a number of years before its theory of operation received much attention in the literature. Early experimenters found that waveguide T junctions having a transversely magnetized ferrite slab suitably placed in the junction could, with proper matching and adjustment of the magnetic field, be changed into circulators. The bandwidth of such devices was very narrow. Refinements producing greater symmetry were found to increase bandwidth so that useful devices were obtained [1]–[4].

More recently a number of papers have appeared in the literature which bear on the theory of operation of the ferrite junction circulator. Auld [5] has considered the theory of symmetrical junction circulators in terms of the scattering matrix of the device. He has shown the necessary relations of the eigenvectors of the matrix, and has indicated how these relations may be obtained. Milano, Saunders, and Davis [6] have applied these concepts in the design of a Y -junction strip-line circulator. Bosma [7], [8], has made an analysis of the strip-line Y -junction circulator in terms of the normal modes of the center disk structure. In his second paper, he shows that the circulation condition is near a degeneracy of a pair of resonances of the disk structure. Butterweck [9] has considered the case of the waveguide junction circulator and has given the waveguide equivalent of Bosma's explanation. Others have attempted explanations based on field displacement, scattering from a post, or surface waves. All of these, if used with proper boundary conditions, conceivably could lead to the same conclusions.

This treatment will consist of an extension of Bosma's approach to the problem. First, we shall present a phenomenological description of the operation of the

Manuscript received July 13, 1964; revised September 8, 1964.
C. E. Fay is with Bell Telephone Labs., Inc., Murray Hill, N. J.
R. L. Comstock is with Lockheed Missiles and Space Co., Research Labs., Palo Alto, Calif. He was formerly with Bell Telephone Labs., Inc., Murray Hill, N. J.